SYNCHROTRON RADIATION

K. Hübner
CERN, Geneva, Switzerland

ABSTRACT

The properties of synchrotron radiation in accelerators and storage rings are presented. The basic steps leading to the most important formulae are outlined in the framework of classical theory. Examples illustrate the importance of this radiation for the design and operation of high energy machines.

1. INTRODUCTION

Accelerated particles emit electro-magnetic radiation. This radiation is especially strong for light particles as electrons or positrons moving on curved orbits in the magnetic guide field of high energy particle accelerators or storage rings.

Detailed accounts of the classical theory of synchrotron radiation and the relevant references can be found in textbooks[1,2,3] or review articles[4,5]. Here we present only a short summary of the main steps in the derivation of the formulae which describe the basic properties of the radiation.

The emphasis is on features which are of interest for the design of circular accelerators. The energy loss suffered by a light particle per turn due to the radiation can become very significant, influencing strongly the choice of the size of the accelerator in the design stage or limiting the maximum energy attainable in a given ring. The radiation has a profound effect on the dynamics of the particles in these machines, leading to damping but also to excitation of oscillations around the equilibrium orbit [3,4,6]. If the radiation is strong enough, the interplay between damping and excitation entirely determines the particle distribution in the circulating bunches [3,4,7].

The radiation properties influence the design of the accelerator components: a powerful RF system is needed to compensate the energy loss per turn, the vacuum system must be designed to cope with the gas desorption from the walls of the beam tube due to the impinging photons, and provisions must be made to remove the heat deposited by the radiation in the vacuum chamber. If the beam energy is sufficiently high, the radiation spectrum extends into the X-ray region and the radiation can penetrate the metallic beam tube. Special shielding must then be added to the vacuum chamber to prevent radiation damage of sensitive accelerator components as electronic equipment, cables and coils. The shielding also reduces the production of noxius gases like O_3 or NO_x by the interaction

of the radiation with the air in the tunnel. Together with the moisture in the air NO_x can form nitric acids which can give rise to corrosion. This must be prevented by proper shielding and ventilation.

Synchrotron radiation has a wide range of applicatons. It is used for beam observation in the accelerators[8] and it provides powerful light and X-ray sources[9]. It also polarizes the particles parallel to the vertical magnetic field in the bending magnets at a useful rate [2,10].

2. LIENARD-WIECHERT POTENTIALS

Introducing the potentials $\vec{A}$, Φ defined by

$$\vec{B} = rot\ \vec{A} \tag{1a}$$

$$\vec{E} = -\,grad\,\Phi - \partial\vec{A}/\partial t \tag{1b}$$

and assuming the Lorentz convention

$$div\ \vec{A} + (1/c^2)\,\partial\Phi/\partial t = 0 \tag{2}$$

yields the wave equations

$$\nabla^2\Phi - (1/c^2)\,\partial^2\Phi/\partial t^2 = -\rho/\varepsilon_o \tag{3a}$$

$$\nabla^2\vec{A} - (1/c^2)\,\partial^2\vec{A}/\partial t^2 = -\vec{j}/(c^2\varepsilon_o) \tag{3b}$$

Consider a point charge e with velocity $c\vec{\beta}(t')$ at $\vec{r}(t')$. It will determine the potentials at the observer being at $\vec{x}$ at a time t. Due to causality

$$t = t' + R(t')/c \tag{4}$$

where R(t') is the distance between particle and observer shown in Fig. 1 together with the unit vector $\vec{n}(t')$. Using the retarded Green's function of equations (3) yields for a moving point charge as source

$$\Phi(\vec{x},t) = \frac{1}{4\pi\varepsilon_o}\iint \frac{e\,\delta[\vec{x}' - \vec{r}(t')]}{R}\,\delta(t' + \frac{R}{c} - t)\,d^3x'\,dt' \tag{5a}$$

$$\vec{A}(\vec{x},t) = \frac{1}{4\pi\varepsilon_o c}\iint \frac{e\vec{\beta}(t')\,\delta[\vec{x}' - \vec{r}(t')]}{R}\,\delta(t' + \frac{R}{c} - t)\,d^3x'\,dt' \tag{5b}$$

After integration the Liénard-Wiechert potentials are obtained

$$\Phi(\vec{x},t) = \frac{e}{4\pi\varepsilon_o}\left[\frac{1}{(1-\vec{n}\vec{\beta})}\,\frac{1}{R}\right]_{ret} \tag{6a}$$

$$\vec{A}(\vec{x},t) = \frac{e}{4\pi\varepsilon_o c}\left[\frac{\vec{\beta}}{(1-\vec{n}\vec{\beta})}\,\frac{1}{R}\right]_{ret} \tag{6b}$$

where the subscript ret means that the terms in the parenthesis must be evaluated at $t' = t - R(t')/c$. For non-relativistic motion, $(1 - \vec{n}\vec{\beta}) \to 1$ and equations (6) exhibit the well-known non-relativistic results.

3. FIELDS OF A POINT CHARGE

Introducing (6) into (1) gives the fields at the observer

$$\vec{B}(\vec{x},t) = (\vec{n} \times \vec{E})/c \tag{7a}$$

$$\vec{E}(\vec{x},t) = \frac{e}{4\pi\varepsilon_o}\left[\frac{(\vec{n}-\vec{\beta})}{(1-\vec{n}\vec{\beta})^3 R^2 \gamma^2}\right]_{ret} + \frac{e/c}{4\pi\varepsilon_o}\left\{\frac{\vec{n}}{(1-\vec{n}\vec{\beta})^3 R} \times \left[(\vec{n}-\vec{\beta})\times\dot{\vec{\beta}}\right]\right\}_{ret} \tag{7b}$$

The first term in in (7b) describes the acceleration independent part of the field. It can also be obtained by considering the static Coulomb field in the rest frame of the particle and by applying a Lorentz transformation to the laboratory system. It shows the familiar R^{-2} dependence.

The second term is proportional to the acceleration $\dot{\beta}$ and describes the "acceleration" field falling off as R^{-1} and being perpendicular to $\vec{n}$. It is this part of the field we are interested in.

4. TOTAL POWER RADIATED

The total power radiated is obtained by integrating Poynting's vector $\vec{S}$ over a sphere around the particle. While the contribution of the acceleration independent part being $\sim R^{-4}$ becomes arbitrarily small for a sufficiently large sphere, the total power due to the "acceleration" fields is independent of the radius of the sphere because of its R^{-2} dependence. Thus, we consider from here on only the acceleration fields.

For non-relativistic velocities (7b) reduces to

$$\vec{E}(\vec{x},t) = \frac{e/c}{4\pi\varepsilon_o}\left[\frac{\vec{n}\times(\vec{n}\times\dot{\vec{\beta}})}{R}\right]_{ret} \tag{8}$$

showing that the radiation is polarized in the plane defined by $\vec{n}$ and $\dot{\vec{\beta}}$. The power received per unit area by the observer is

$$\vec{S} = \vec{E}\times\vec{B} = \varepsilon_o c E^2 \vec{n}$$

and the power per solid angle becomes

$$\frac{dP}{d\Omega} = |\vec{S}|R^2 = \left(\frac{e}{4\pi}\right)^2 \frac{1}{\varepsilon_o c}\,\dot{\beta}^2 \sin^2\Theta \tag{9}$$

Fig. 2 shows the geometry. By integrating over the solid angle the Larmor formula for the total radiation power is obtained

$$P = \frac{e^2}{6\pi\varepsilon_o c}\,\dot{\beta}^2 \tag{10}$$

valid for $\beta \ll 1$.

After a Lorentz transformation of both sides of (10) to the laboratory system the general formula becomes

$$P = \frac{e^2}{6\pi\varepsilon_o c^3}\,\gamma^4\left(\gamma^2\dot{v}_{pa}^2 + \dot{v}_{pe}^2\right) \tag{11}$$

where $\dot{v}_{pa}$ is parallel to $\vec{v}$ and $\dot{v}_{pe}$ is perpendicular to it. If the acceleration $\dot{v}_{pe}$ is due to the curvature of the orbit (11) can be written as

$$P = \frac{e^2}{6\pi\varepsilon_o c}\left(\frac{\dot{\gamma}^2}{\beta^2} + \frac{c^2\beta^4\gamma^4}{\rho^2}\right) \tag{12}$$

where ρ is the radius of curvature. Writing (11) in terms of momenta shows that the same accelerating force, i.e.

$$\dot{p}_{pa} = \dot{p}_{pe}$$

produces a γ^2 times stronger radiation power if applied in perpendicular direction rather than in parallel direction. As examples will show, the first term in (12) can be neglected under the conditions prevailing in accelerators. Hence, we shall consider further only the power radiated due to the curvature of the orbit

$$P_\gamma = \frac{e^2 c}{6\pi\varepsilon_o}\,\frac{\beta^4\gamma^4}{\rho^2} \tag{13}$$

Integrating over the circumference L of the accelerator the energy loss per turn is obtained

$$U_o = \int_o^L \frac{P_\gamma}{\beta c}\,ds \approx \frac{2}{3} r_o m_o c^2 \beta^3\gamma^4 \int_o^L \frac{ds}{\rho^2} \tag{14a}$$

with the classical radius of the particle

$$r_o = \frac{1}{4\pi\varepsilon_o}\,\frac{e^2}{m_o c^2}$$

If the machine has a constant bending radius (isomagnetic machine) we get from (14a)

$$U_o = \frac{4\pi}{3} r_o m_o c^2 \beta^3\gamma^4/\rho \tag{14b}$$

Table I gives some examples demonstrating the importance of synchrotron radiation for the design of circular machines. We consider two extreme cases of e± storage rings: DCI[11] operating since 1976 at LAL in Orsay (France) and LEP[12] under construction at CERN. The last line refers to LHC[13], a Large Hadron Collider (pp or pp-bar), which

could possibly be installed above the LEP ring in the LEP tunnel. This case is added to show that synchrotron radiation becomes discernible in proton machines only at the highest energies, the reason being the strong γ dependence of P_γ. Although P_γ appears to be very small in LEP, the total power radiated by both beams, each containing N particles, after averaging over one revolution period T_o

$$P_{rad} = 2NU_o/T_o \qquad (15)$$

can become very substantial as Table I shows.

The total loss per turn is proportional to 2N because the radiation is incoherent. The emission of radiation from each particle is independent from the emission by other particles. The reason is that most other companion particles in a bunch are in the far-zone of the radiation emitted by the relativistic particle under consideration. The particles in the near-zone, which can together emit coherent light, are too few because the near-zone has a very small extension[14]. In LEP, for example, only 10^{-8} of the particles in a bunch are in the near-zone.

Table I, Examples of energy loss and radiated power

	E (GeV)	ρ(m)	U_o (MeV)	P_γ (μW)	$N/10^{12}$	P_{rad} (MW)
DCI[a] e±	1.8	3.8	0.24	0.49	0.17	0.04
LEP e±	55	3100	260	0.64	1.6	1.5
"	100	3100	2800	7.0	1.6	16
LHC p	8100	3100	0.011	3.10^{-5}	48	0.002

a) Only horizontal bends considered.

It is apparent from the table that in large electron-positron storage rings a powerful RF system is needed to compensate U_o and P_{rad} despite the very large bending radius. As a matter of fact, the bending radius in LEP is chosen so large (bending field only 0.11 T at 100 GeV) in order to limit the amount of synchrotron radiation. The precise value of ρ is the result of a cost optimisation assuming operation in the 90 GeV range and weighing tunnel and magnet cost against the cost of a RF system which uses copper cavities[15]. While the RF system in DCI consists of two cavities and two transmitters (2 x250 kW), the RF system of LEP in phase I (55 GeV) consists of 128 copper cavities, each 2.5 m long, and of 16 klystrons delivering each 1 MW in CW operation. The difference between the total RF power installed and P_{rad} given in the table is the power dissipated in the cavity walls due to ohmic losses. Obviously, at higher energy, there is a strong incentive to replace the copper cavities by superconducting cavities, which provide a higher acceleration gradient ($\approx$ 5MV/m)[16] and have vanishing dissipation in the cavity walls. This will lead to a more compact and more efficient RF system once all technical problems are overcome.

The power emitted per unit length in the dipole magnets by both beams becomes 1 kW/m in LEP at 100 GeV, indicating that synchrotron radiation will profoundly influence also the design of the vacuum system.

Finally, we compare the radiated power due to acceleration perpendicular to the velocity in the LEP dipole magnets to the power radiated during acceleration in the copper RF cavities providing about 0.8 MeV/m. Using (12) we obtain 6×10^{12} for this ratio! Next we consider the radiation due to parallel acceleration in a linac. For example, the power radiated by an accelerated electron in the 2.3 GeV linac at LAL is 2×10^{-17} W leading to a total energy loss of only 8.5×10^{-14} GeV per electron during the acceleration from about 100 keV to 2.3 GeV in the 230 m long linac, which again illustrates that parallel acceleration creates very little radiation. Hence, it is indeed admissible to neglect the first term in (12) when considering radiation in accelerators.

5. ANGULAR DISTRIBUTION OF POWER

By virtue of (7) the instantaneous power measured at the observation point is

$$[\vec{S}.\vec{n}]_{ret} = \frac{e^2}{16\pi^2\varepsilon_0 c}\left\{\frac{1}{(1-\vec{n}\vec{\beta})^6 R^2}\,|\vec{n}\times[(\vec{n}-\vec{\beta})\times\dot{\vec{\beta}}]|^2\right\}_{ret} \qquad (16)$$

The denominator in the brackets governs the behaviour as it determines the strong peaking of the radiation pattern around $\vec{\beta}$ for relativistic particles, while the numerator in the brackets gives the fine structure of the pattern which is of a little interest as it can practically not be resolved.

It is instructive to consider the power radiated by the particle per unit solid angle in terms of its own time t'. For $\gamma \gg 1$

$$\frac{dP(t')}{d\Omega} \approx \frac{e^2}{2\pi^2\varepsilon_0 c}\,\dot{\beta}^2\,\frac{\gamma^6}{(1+\gamma^2\vartheta^2)^3}\left[1-\frac{4\gamma^2\vartheta^2\cos^2\varphi}{(1+\gamma^2\vartheta^2)^2}\right] \qquad (17)$$

The geometry is defined in Fig. 3. It is evident from (17) that the radiation is confined to a narrow cone around $\vec{\beta}$ where $\theta < 1/\gamma$. The rms angle of the distribution is independent of ρ. It becomes

$$\vartheta_{rms} = 1/\gamma \qquad (18)$$

Its numerical value is 284 μrad for DCI and 10 μrad for LEP (55 GeV).

6. FREQUENCY SPECTRUM

The radiation pattern is as if the particle had a searchlight fastened to it, pointing in the direction of motion. In order to see something, the observer must be close to the median plane (x,s) of the accelerator and, for an orbit with only positive curvature, outside the area bound by the closed orbit. The radiation will be visible to him only when emitted on the arc AB as indicated in Fig. 4. The duration of this flash of light is equal to the difference in travel time of the particle and the radiation between A and B.

$$\Delta t = t_p - t_r \approx \rho / c \gamma^3 \tag{19}$$

Therefore, the frequency spectrum of the radiation will start to drop at

$$\omega = 1/\Delta t \approx c \gamma^3 / \rho \tag{20}$$

This frequency corresponds to soft X-rays in DCI; to conventional X-rays in LEP when operating at 55 GeV; to hard X-rays in LEP at 100 GeV, and to VUV radiation in LHC.

Since the particle motion is periodic, the observer will see a line spectrum; the line spacing and the lowest frequency are given by the revolution frequency.

Considering the total energy incident on the observer per particle passage

$$\frac{dW}{d\Omega} = \int R^2 |\vec{S}| \, dt$$

and using Fourier transform techniques yields

$$\frac{d^2W(\omega,\vartheta)}{d\omega \, d\Omega} = \frac{e^2}{12\pi^3 \varepsilon_0 c} \left(\frac{\omega\rho}{c}\right)^2 \frac{(1+\gamma^2\vartheta^2)^2}{\gamma^4} \left[K_{\frac{2}{3}}^2(\xi) + \frac{\gamma^2\vartheta^2}{1+\gamma^2\vartheta^2} K_{\frac{1}{3}}^2(\xi)\right] \tag{21}$$

the energy received by the observer per unit solid angle and per unit frequency interval during a single passage of one particle, The geometry is given in Fig. 5. Note that the definition of θ is different from the one given in Fig. 3. The origin is defined uniquely by the position of the observer relative to the orbit. Equation (21) includes not only the radiation emitted by the particle when it is at the origin but also radiation from all other points on the trajectory which are sufficiently close to the origin such that some of the radiation emitted can illuminate the observer.

The argument of the modified Besselfunctions K is

$$\xi = \frac{\omega}{2\omega_c} (1+\gamma^2\vartheta^2)^{3/2} \tag{22}$$

where ω_c is the so-called critical frequency

$$\omega_c = \frac{3}{2} \frac{c\gamma^3}{\rho} \tag{23}$$

which is equal to (20) except the numerical factor 3/2 chosen for reasons explained later. Since

$$K \sim e^{-\xi}/\xi \qquad \text{for } \xi \gg 1$$

we expect that the radiation is confined to a decreasingly smaller range in θ for increasing ω. This is illustrated in Fig. 6.

The first term in the bracket of (21) corresponds to the polarization of the radiation in the plane of the orbit, the second term describes polarization perpendicular to this plane. Integrating over all frequencies yields

$$\frac{dW(\vartheta)}{d\Omega} = \frac{7e^2}{64\pi\varepsilon_0} \frac{1}{\rho} \frac{\gamma^5}{(1+\gamma^2\vartheta^2)^{5/2}} \left[1 + \frac{5}{7} \frac{\gamma^2\vartheta^2}{(1+\gamma^2\vartheta^2)}\right] \tag{24}$$

The relative contributions of the two polarizations to the energy received by the observer is shown in Fig. 7. It can be seen that the polarization parallel to the plane of the orbit dominates. Integration of (24) over θ yields for the ratio of the contributions

$$W_{pe}/W_{pa} = 1/7 \tag{25}$$

showing again the dominance of the polarization in the orbital plane.

A more relevant quantity for the design of an accelerator is the power radiated by the particle at frequencies between ω and ω + dω. This quantity can be obtained from (21). Imagine the particle on a circular orbit with radius ρ and the whole orbit enclosed in a large sphere centered at the origin of Fig. 5. Integrating over all angles gives for the energy in the frequency interval ω, ω + dω received by the sphere per turn

$$\int d^2W/(d\omega\, d\Omega)\; d\Omega = (d\,W/d\omega)_{turn}$$

Dividing by the revolution time yields the power emitted between ω and ω + dω

$$\frac{dP_\gamma}{d\omega} = \frac{\beta c}{2\pi\rho}\left(\frac{dW}{d\omega}\right)_{turn}$$

$$\frac{dP_\gamma}{d\omega} = \frac{P_\gamma}{\omega_c}\; S\left(\frac{\omega}{\omega_c}\right) \tag{26}$$

where

$$S = \frac{9\sqrt{3}}{8\pi}\left(\frac{\omega}{\omega_c}\right)\int_{\omega/\omega_c}^{\infty} K_{\frac{5}{3}}\left(\frac{\omega}{\omega_c}\right)\, d\left(\frac{\omega}{\omega_c}\right) \tag{27}$$

is a universal function shown in Fig. 8. Combining

$$\int \frac{dP_\gamma}{d\omega}\, d\omega = P_\gamma$$

with (26) shows that the area under the curve $S = S(\omega/\omega_c)$ is unity. The numerical factor in (23) defining ω_c is chosen so that the line $\omega/\omega_c = 1$ divides this area into two equal parts. Hence, half of the power is emitted with frequencies above ω_c, the other half with frequencies below ω_c. Beware, some text books (e.g. ref. 1) use a different numerical factor in (23). The function S has a maximum at about $\omega/\omega_c = 1/3$. From the asymptotic behaviour of the Besselfunction in (27)

$$\text{for } \omega/\omega_c \ll 1 \qquad S \simeq 1.34\ (\omega/\omega_c)^{1/3} \tag{28}$$

$$\text{for } \omega/\omega_c \gg 1 \qquad S \simeq 0.77\ (\omega/\omega_c)^{1/2}\ \exp\ (-\omega/\omega_c)$$

7. QUANTUM EMISSION

The emission of radiation at frequency ω is equivalent to the emission of quanta with energy

$$u = h\omega/2\pi$$

where h is Planck's constant. The number of quanta n(u) emitted per unit time with energies between u and u + du can be obtained from

$$u\, n(u)\, du = \frac{dP_\gamma}{d\omega}\, d\omega$$

leading to

$$n(u) = \frac{P_\gamma}{u_c^2}\, F(u/u_c) \tag{29}$$

with the critical energy u_c defined by

$$u_c = \hbar\omega_c / 2\pi \tag{30}$$

The shape of the spectrum is determined by the univeral function F shown in Fig. 8 and related to S by

$$F(\omega/\omega_c) = \frac{\omega_c}{\omega}\, S(\omega/\omega_c) \tag{31}$$

The average rate of emission becomes

$$N_\gamma = \int_0^\infty n(u)\, du$$

$$N_\gamma = \frac{15\sqrt{3}}{8}\, \frac{P_\gamma}{u_c} \approx 3.25\, P_\gamma / u_c \tag{32}$$

The actual rate fluctuates. Inspecting a large example of measurements of N_γ would reveal a Poisson distribution with the mean given by (32). The mean quantum energy is

$$\langle u \rangle = \frac{8}{15\sqrt{3}}\, u_c \approx 0.308\, u_c \tag{33}$$

The average number of quanta emitted on a circular orbit per radian depends only on γ

$$N_\gamma \frac{\rho}{\beta c} = \frac{5}{2\sqrt{3}}\, \frac{\gamma}{137} \approx \frac{\gamma}{100} \tag{34}$$

Table II gives some examples. As said before, the radiation in small storage rings is typically in the soft X-ray region, e.g. the critical energy u_c in DCI corresponds to the K-line excitation of calcium. This radiation cannot penetrate the vacuum chamber. In the large storage rings as PEP, PETRA and LEP the radiation energy gets into the γ-ray range. For comparison, Co_{60} emits γ-rays at 1.2 and 1.3 MeV. Lead shielding around the vacuum chamber is needed to protect sensitive accelerator components.

Table II, Examples of critical energy and emission rate

	E (GeV)	u_c(keV)	N_γ/c (m^{-1})
DCI[a] e±	1.8	3.4	10
LEP e±	55	119	0.37
	100	715	0.66
LHC p	8100	0.06	0.03

Fig. 9 shows a cross-section of the vacuum chamber in the LEP dipoles and quadrupoles with its lead shield. The radiation originating in the quadrupoles ($u_c \approx 10$ keV at 55 GeV) is rather weak because it is only due to particles not going through the centre of the quadrupoles. Nevertheless, lead shielding is also required around the quadrupole

chambers as well as around all other beam tubes close to the dipoles because the radiation emitted near the dipole ends and being parallel to $\vec{\beta}$ can illuminate the beam tube over a a long distance downstream of the dipoles.

The LEP vacuum chambers are made from aluminium to facilitate heat conduction between the surface where the radiation impinges and the cooling channel. The surface directly illuminated by the beam is a narrow strip as high as the beam on the inner wall next to the cooling channel. A sizeable fraction of the radiation is scattered and deposits energy outside the narrow strip. In LEP phase I only the cooling channel opposite the pump and in the median plane is used. The two cooling channels close to the pump will be used at higher energy.

The third column in Table II gives the number of photons emitted by a single particle per unit length. Multiplying with the number of particles in the beam given in Table I shows that the vacuum chamber is bombarded by an enormous amount of powerful photons which can cause a strong gas desorption. Although the radiation is very effective in cleaning the vacuum system, provided the vacuum pumps can remove the gas load, it is obvious that the initial cleanliness of the system must be sufficiently good to allow for a reasonable beam lifetime. Otherwise the beam kills itself by the self-generated pressure rise without ever getting round to the cleaning of the vacuum walls. Although the energy of the photons is very low in LHC, the number of photons released by the beams is as high as in LEP. Hence, careful attention must be paid also there to the cleanliness of the vacuum chamber.

* * *

REFERENCES

1) J.D. Jackson, Classical Electrodynamics, Wiley, New York (1962)

2) A.A. Sokolov and I.M. Ternov, Synchrotron Radiation, Berlin, Akademie-Verlag (1968)

3) H. Bruck, Accélérateurs circulaires de particules, Presses Universitaires de France, Paris (1966)

4) M. Sands, report SLAC-121 (1970) published in Proc. Int. School "Enrico Fermi", 46th course, Varenna 1969; B. Touschek (ed.); Academic Press, New York 1971.
M. Sands, report SLAC-121 Addendum (1979).

5) A. Hofmann, Physics Reports 64 (1980) 253

6) K. Hübner, these proceedings

7) A. Piwinski, these proceedings

8) A. Hofmann, IEEE Trans. on Nucl. Sci., NS-28 (1981) 2132

9) S. Tazzari, these proceedings

10) B.W. Montague, Physics Reports 113 (1984) 1

11) P. Marin, Proc. IXth Int. Conf. on High Energy Accelerators, Stanford (1974) 49

12) LEP Design Report, Vol. II, CERN-LEP/84-01 (1984)

13) M. Jacob (editor), Proc. of the ECFA-CERN Workshop on a Large Hadron Collider in the LEP tunnel, 21.-27. March 1984, Lausanne and Geneva, Vol. I, ECFA 84/85, CERN 84-10 (1984)

14) A.A. Sokolov and I.M. Ternov, Izv. VUZ, Fiz. 10 (1967) 66

15) The LEP Study Group, CERN/ISR-LEP/79-33 (1979)

16) H. Piel, Proc. 12th Intern. Conf. on High-Energy Accel., Batavia (1983) 571

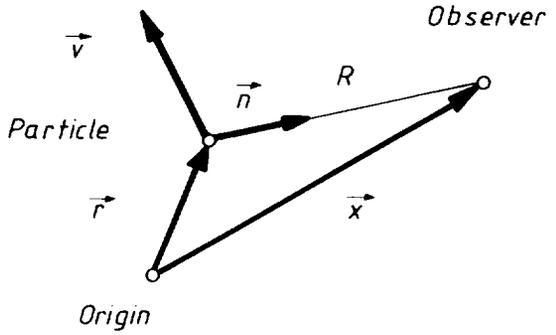

Fig. 1 Relative position of observer and radiating particle

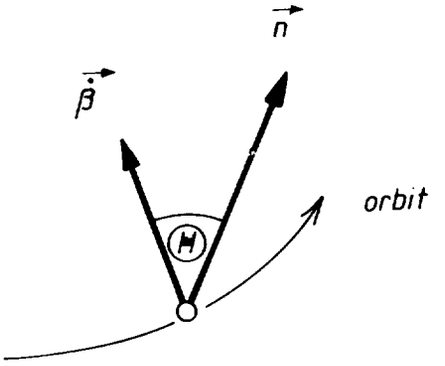

Fig. 2 Definition of angle θ

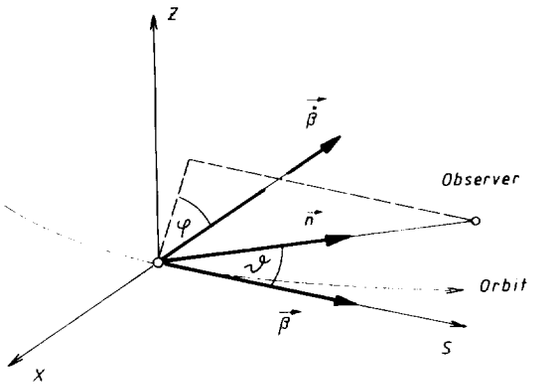

Fig. 3 Definition of angles θ and ϕ

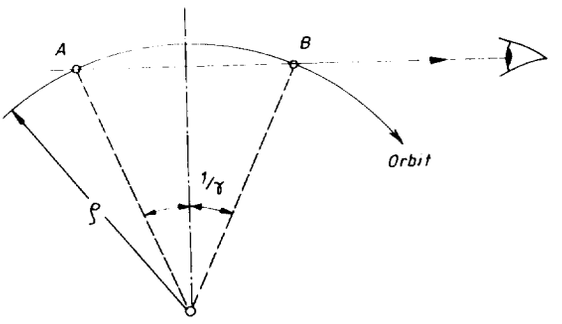

Fig. 4 Part of the trajectory from where emitted light can reach the observer

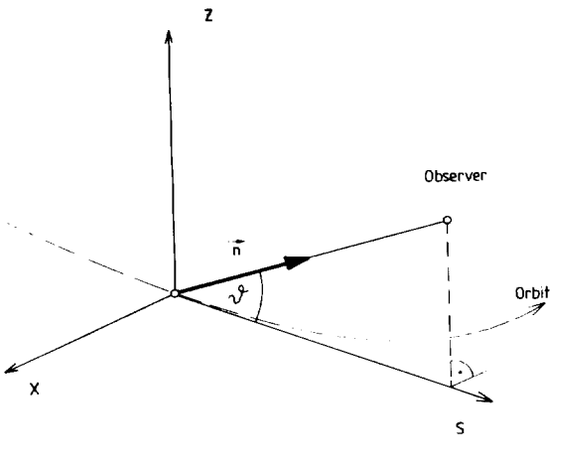

Fig. 5 Definition of angle θ

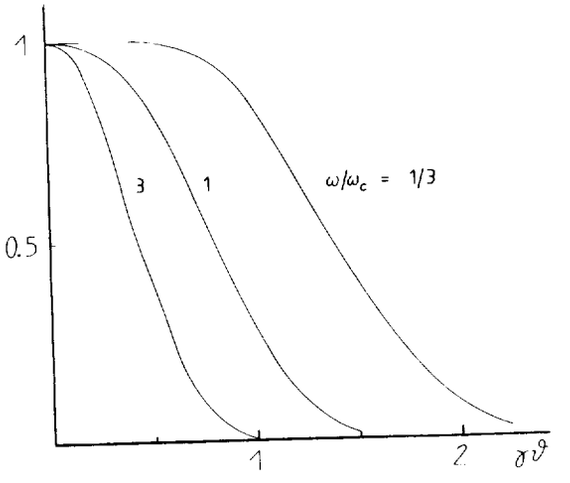

Fig. 6 Energy received by the observer per unit solid angle, per unit frequency interval, and per particle passage versus angle in arbitrary units. Parameter is the normalized frequency of the radiation.

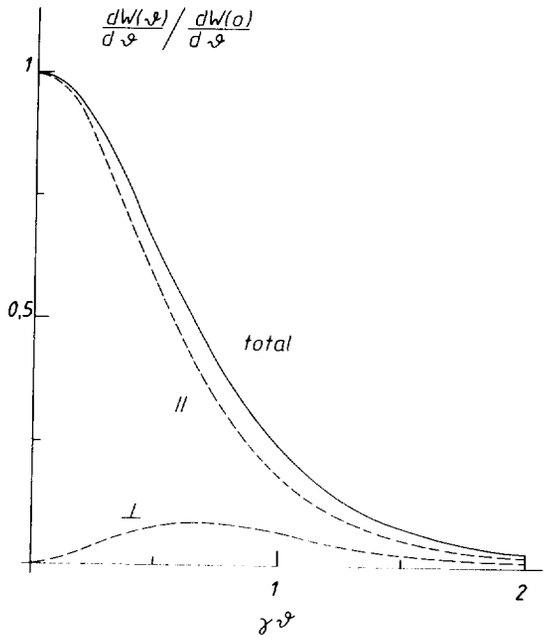

Fig. 7 Contribution of the two polarizations to the energy, received by the observer per unit solid angle and per particle passage, versus angle. The polarization direction indicated is relative to the plane of the orbit.

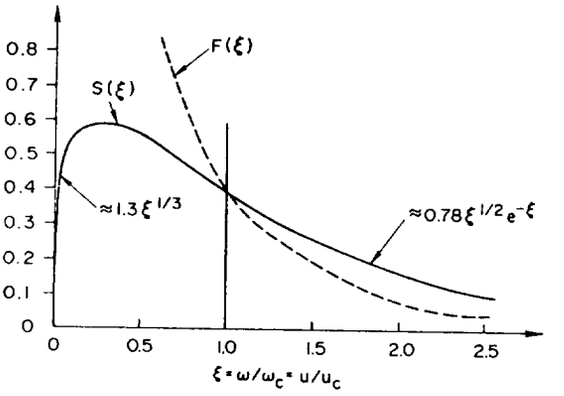

Fig. 8 Normalized power spectrum S and photon number spectrum $F^{4)}$

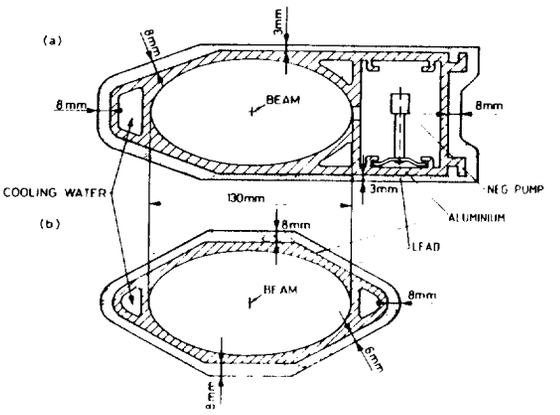

Fig. 9 Cross-section of the LEP vacuum chamber in the dipoles (a) and in the quadrupoles (b) with its lead shield.